HHS Public Access

Author manuscript

Gene Ther. Author manuscript; available in PMC 2016 September 10.

Published in final edited form as:

Gene Ther. 2016 May ; 23(5): 415–423. doi:10.1038/gt.2016.12.

Hair cell stereociliary bundle regeneration by espin gene transduction after aminoglycoside damage and hair cell induction by Notch inhibition

Akiko Taura[1], **Kojiro Taura**[2], **Yukinori Koyama**[2], **Norio Yamamoto**[1], **Takayuki Nakagawa**[1], **Juichi Ito**[1], and **Allen F. Ryan**[3]

[1]Department of Otolaryngology-Head and Neck Surgery, Graduate School of Medicine, Kyoto University, Kyoto 606-8507, Japan

[2]Department of Surgery, Graduate School of Medicine, Kyoto University, Kyoto 606-8507, Japan

[3]Departments of Surgery/Otolaryngology and Neurosciences, UCSD School of Medicine, La Jolla, CA 92093 USA and the VA Medical Center, San Diego, CA 92161 USA

Abstract

Once inner ear hair cells (HCs) are damaged by drugs, noise or aging, their apical structures including the stereociliary arrays are frequently the first cellular feature to be lost. While this can be followed by progressive loss of HC somata, a significant number of HC bodies often remain even after stereociliary loss. However, in the absence of stereocilia they are nonfunctional. HCs can sometimes be regenerated by Atoh1 transduction or Notch inhibition, but they also may lack stereociliary bundles. It is therefore important to develop methods for the regeneration of stereocilia, in order to achieve HC functional recovery. Espin is an actin bundling protein known to participate in sterociliary elongation during development. We evaluated stereociliary array regeneration in damaged vestibular sensory epithelia in tissue culture, using viral vector transduction of two espin isoforms. Utricular HCs were damaged with aminoglycosides. The utricles were then treated with a γ-secretase inhibitor, followed by espin or control transduction and histochemistry. While γ-secretase inhibition increased the number of HCs, few had stereociliary arrays. In contrast, 46 hrs after espin1 transduction, a significant increase in hair-bundle-like structures was observed. These were confirmed to be immature stereociliary arrays by scanning electron microscopy. Increased uptake of FM1–43 uptake provided evidence of stereociliary function. Espin4 transduction had no effect. The results demonstrate that espin1 gene therapy can restore stereocilia on damaged or regenerated HCs.

Keywords

Hair cell regeneration; Stereocilia regeneration; espin; notch inhibition

Address correspondence and offprint requests to: Allen F. Ryan, Ph.D., Division of Otolaryngology, 0666, School of Medicine, 9500 Gilman Drive, La Jolla, CA 92093 USA, Tel.: 534-4659, Fax: 534-3094, ; Email: afryan@ucsd.edu

COMPETING INTERESTS

The authors declare that they have no competing financial interests.

INTRODUCTION

Hearing and balance disorders are important causes of disability in patients. The major cause is sensory hair cell (HC) loss in the inner ear.[1] In the damaged sensory epithelia of birds, new HCs regenerate in both the vestibular[2] and auditory sense organs.[3] However, in mammals, HC loss is irreversible. For this reason, the regeneration of HCs in mammals is a subject of considerable research. Successful regeneration of functional HCs in mammals would be a major advance in the therapy of inner ear disorders.

When HCs are damaged, apical structures including stereociliary bundles are often the first cellular elements to be lost.[4] The stereociliary bundle, as the site of mechanotransduction, is critical for HCs to maintain their physiological function. Some of these bundleless HCs can survive for considerable periods of time, but spontaneous stereociliary regeneration is not normally observed.[5] So the replacement of stereocilia on surviving HCs is a potential strategy for functional recovery following inner ear sensory cell damage.

The espins are a family of actin bundling proteins, produced in multiple isoforms from a single gene (*espn*). They are localized in the stereocilia of HCs as well as the microvilli of many sensory cells.[6] Espins are associated with the parallel actin bundles of stereocilia throughout stereocilia formation during development.[7–8] Stereocilia are hypoplastic in the absence of the *espn* gene, exhibiting reduced length and abnormal structure. This results in hearing loss and vestibular dysfunction in the *Jerker* mouse model[9] and in the human DFNB36 deafness mutation.[10] Given its critical role in stereociliary development, we reasoned that induced espin expression might be useful for stereociliary bundle regeneration.

Gene therapy has been found to be a promising tool for application to the inner ear. The labyrinth is anatomically well suited to local gene therapy, because it is a closed system that is isolated from other organs and is relatively easy to access via the middle ear, thus allowing local application and relative isolation of viral vectors with minimal spread to other sites.[11] Recently, a degree of success has been reported using experimental gene therapy for various types of inner ear disorder caused by ototoxic drugs and genetic abnormalities.[12_14]

With respect to HC regeneration, techniques which recapitulate the developmental program of HCs have generally been employed. These can, under the appropriate circumstances, induce nonsensory cells to convert to HCs with or without cell division.[15_19] One of the earliest steps in HC specification is induction of the basic helix-loop-helix transcription factor ATOH1 by EYA1 and SIX1.[20] ATOH1 interacts with the Notch signaling system to form the mosaic of HCs and supporting cells, with Notch ligands suppressing the production of ATOH1 in the latter.[21] The transduction inner ear supporting cells with the *atoh1* gene has been reported to be effective in inducing HC formation, especially in developing mammals.[22] Blockade of Notch signaling using γ-secretase inhibitors has also been shown to be effective in mammalian HC induction, since Notch signals act on supporting cells to inhibit their differentiation into HCs. Several studies have reported the conversion of supporting cells into HCs following Notch inhibition.[23_25] The transdifferentiation process in the neonatal utricle is characterized by both mitotic and non-mitotic processes.[21,26] Loss

of HCs induces generally modest spontaneous regeneration due to loss of Notch inhibition of supporting cells. Notch inhibitors greatly enhance this process, inducing some supporting cells to dedifferentiate, enter the cell cycle, and produce daughter cells which can assume either a supporting cell or HC phenotype. Other supporting cells de-differentiate and transdifferentiate directly into HCs. However, in many cases regenerated HCs are immature and exhibit no or only partial function.[23,25,27]

These prior studies suggest that enhancing the growth of stereocilia may be a useful means by which to restore cochlear function following HC damage and/or regeneration. In the present study, we examined the potential for *espn* gene transduction to induce the regeneration of functional stereociliary arrays, following ototoxic HC damage and HC regeneration induced by Notch inhibition. We evaluated viral vector transduction with Espin1 or Espin4, both linked to GFP. A GFP-only vector was used as a control.

RESULTS

Gentamicin damage to the HC stereociliary bundles and cell bodies

We evaluated the number of HC somata and stereociliary bundles after gentamicin (GM) treatment of utricular maculae *in vitro* (Figure 1). After GM treatment, stereocilliary bundles were almost entirely lost from the macular epithelium (Figure 1D) and the number of HC bodies was dramatically decreased. However, after an initial steep decline in HCs, the number was stable out to 10 days. Thus, a subset of HC somata, absent their stereocilia, remained even 10 days after GM damage (Figure C).

Transduction of macular explants

We examined the transduction of GM-treated macular explants by Adenovirus-GFP (Ad-GFP), Ad.E1-EGFP (Ad-E1) and Ad.E4-EGFP (Ad-E4) adenoviral vectors. The maculae were well transduced by each vector, and the efficiencies of the three transductions were similar. Both HCs and supporting cells were transduced (Figure 2). The expression of GFP in Ad-GFP transduced cells was diffused throughout the cell bodies (Figure 2A). In contrast, filamentous patterns of GFP were observed in Ad-E1 and Ad-E4 transduced cells (Figure 2B, 2C). These expression patterns appeared to be related to the actin-binding characteristics of *espin*.

The effect of DAPT treatment

As noted above, after GM damage, the number of HCs present in macular explants decreased dramatically (Figure 3A, 3A', 3B,3B'). However, damaged explants treated with DAPT exhibited substantially more cells expressing the HC marker myosin7A, especially at the edges of the explants. In sectioned samples, these myosin7A-positive cells were observed to lie primarily in the supporting cell layer (Figure 3C, 3C'). The number of myosin7A-positive cells in GM damaged explants and DAPT-treated explants were respectively: 25.4 ± 5.5 (SD) and 38.5 ± 8.64 (SD) / 10000 μm^2 ($P < .05$, t test). However, stereociliary bundles remained very sparse in the DAPT-treated explants (data not shown).

Time-lapse microscopy after adenoviral transduction

Espin1-GFP expression after Ad-E1 transduction of GM-damaged, DAPT-treated explants was examined by time-lapse microscopy. Twenty-four hrs after vector administration, almost no GFP-positive cells were observed (Figure 4A). However, by 31 hrs, GFP expression had increased. By 46–48 hrs, expression reached a visual maximum and extensive filamentous GFP expression was observed (Figure 4B, 4C, arrows). GFP expression then declined, but remained apparent for an additional 24 hrs. GFP signals following transduction with the other 2 adenoviruses (Ad-GFP and Ad-E4) increased, peaked, and declined at a slightly earlier stage (data not shown).

Influence of *espin* gene transduction on stereociliary bundles

Transduction of damaged and regenerated explants with Ad-GFP or Ad-E4 had no effect on the number of stereociliary bundles. However, on the surfaces of Ad-E1 transduced explants a large increase in the number of phalloidin-positive structures which resembled immature stereociliary bundles was noted (Figure 5A). In sectioned explants, the many myosin7A-positive cells that were apparent in the supporting cell layer exhibited GFP-positive extensions that reached from the supporting cell layer to the apical surface of the epithelium. Moreover, phalloidin-labeled stereociliary bundle-like structures projected from the apical surfaces of these extensions (Figure 5B). While some stereociliary bundles were observed in Ad-GFP- or Ad-E4-transduced explants (11.4 ± 6.87 (SD) / 10000 μm^2), a substantially and significantly greater number were observed on Ad-E1-transduced macular explants (28.8 ± 7.82 (SD) / 10000 μm^2; .P < .05, t-test) (Figure 5C).

Scanning electron microscopy (SEM)

After Ad-GFP transduction, the reticulated boundaries between cells were clearly apparent on the surfaces of explants imaged by SEM. Small microvilli and basal bodies were also observed on the surfaces of the cells, but stereociliary bundles were essentially absent (Figure 6A). In contrast, on the surface of Ad-E1 transduced explants, many immature stereociliary bundle-like structures were observed (Figure 6B). However, there were very few immature stereociliary bundle-like structures in Ad-E4 transduced explants, although elongated microvillus-like elements were seen (Figure 6C). When the stereociliary bundle-like structures were quantified, the number on Ad-E1 transduced explants was substantially and significantly ($p < .05$, t-test) greater than in Ad-GFP or Ad-E4 transduced epithelia (Figure 6D). Higher magnification images revealed recognizable bundles of stereocilia, with a typical stair-step arrangement, on Ad-E1 transduced explants. These bundles exhibited a single, central kinocilium, and stereocilia were present on approximately one half of the apical surface of each bundle-bearing cell (Figure 7A). These stereocilia appeared to be linked at their tops (Figure 7B).

Functional analysis of stereociliary bundles using FM1–43FX loading

After brief treatment with FM1–43FX, only a small number of fluorescent cells were observed in Ad-GFP and Ad-E4 transduced explants (Figure 8A, 8C). However, substantially more FM1–43FX-positive cells were observed in Ad-E1 transduced explants (Figure 8B). Quantitative analysis of FM1–43 positive cells in explants revealed dramatic

and significant ($p < .05$) differences in labeling between Ad-E1 transduced explant and those transduced with either Ad-GFP or Ad-E4 (Figure 8D). These results provide strong evidence that stereociliary bundles on Ad-E1 transduced explants exhibit functional mechanoelectrical transduction channels.

DISCUSSION

Gene therapy has proven to be a promising tool for the correction of gene deficiencies and for introducing beneficial gene expression into a variety of tissues. Recently, advances have been reported in the use of gene therapy for inner ear disorders.[12] In this study, we evaluated the potential for gene therapy-induced espin overexpression to regenerate HC stereociliary bundles after HC damage and induction. When HCs were damaged with aminoglycosides, their apical surface including the hair bundle was rapidly lost, as has been previously reported.[4] This was followed by the degeneration of the HC soma for most cells. However, a subpopulation of HCs survived, absent their stereocilia, even at 10 days post aminoglycoside treatment. Again, this has been reported in prior studies.[e.g. 19] Treatment of damaged cultures with the γ-secretase inhibitor DAPT resulted in the generation of additional HCs, but these cells lacked stereociliary bundles in our study. This agrees with the results of some prior evaluations of HC regeneration,[17,19] although stereocilia have been reported on regenerated mammalian HCs in other studies, especially when longer periods of regeneration are involved.[e.g. 15, 18] Transduction with Espin1-EGFP in an adenoviral vector led to robust growth of stereociliary bundles, while transduction with an Espin4-EGFP or GFP alone was ineffective.

As noted above, espins are actin bundling proteins produced in multiple isoforms from a single gene. Espin mutant mice show abnormal stereocilia, indicating the importance of this gene for these structures.[9] Moreover, specific espin isoforms have the potential to be differentially involved in stereociliogenesis during HC development. In the inner ear HCs of altricial rodents, the espin1 isoform accumulates during the late embryonic and early postnatal periods, while the espin2 and 3 isoforms predominate in the embryonic inner ear until approximately E20. Therefore, espins1–3 are candidates for involvement in stereociliagenesis, with espin1 expression most closely matching the period of stereociliary development.[9] In contrast, the espin4 isoform accumulates between postnatal days 6 and 10, after stereocilia have reached their essentially adult characteristics.[9] This suggests that espin4 is less likely to be involved in stereociliagenesis. However, when espin4 is over-expressed in other cell types, microvilli are elongated[23] and in cochlea both microvilli and stereocilia are similarly elongated.[24] Therefore, more than one espin isoform has the capacity to influence stereocilia formation. We therefore tested the ability of espin1 and espin4 overexpression to generate stereocilia in damaged and regenerated HCs. In Ad-E1 transduced explants, we observed phalloidin-positive stereocilia bundle-like structures on myosin7A-positive cells. SEM study revealed that only in Ad-E1 transduced explants did we observe recognizable stereocilia with a staircase pattern. This, in combination with the data cited above, suggests that espin4 may be more involved in the elongation than in the genesis of stereocilia. However, it should of course be noted that the fusion of espin4 to GFP might have altered its properties in our experiments. Any conclusions regarding the lack of effect of espin4 transduction on stereociliary bundle formation should keep this in mind.

These results suggest that espin1 gene therapy might be effective as a means of regenerating stereociliary bundles. However, it does not necessarily follow that the stereocilia are functional. Rapid FM1–43 accumulation in HCs, on the order of seconds, is thought to be mediated by entry through functional mechanoelectrical transduction channels.[25,26] Although endocytotic entry has been reported in guinea pig inner HCs, this occurs with substantially slower kinetics.[27] Therefore, rapid FM1–43 loading is thought to reflect the physiological function of HC mechanotransduction channels at the tips of the stereocilia.[26]. In Ad-E1 transduced explants, the number of FM1–43 positive cells observed after brief exposure was substantially and significantly ($p < .05$, t-test) larger than the other two experimental groups. This suggests that stereocilia induced by espin1 gene therapy bear functional MET (mechanoelectrical transduction) channels.

The fact that espin1 overexpression alone increased the formation of stereociliary arrays is perhaps surprising, given that actin-crosslinking presumably represents only part of the process required for stereociliary formation. This suggests that the genetic program for stereociliagenesis is partially active in damaged and/or regenerated HCs, but lacks *espn* gene expression as a critical component. The reason for this lack is unclear. It can be assumed that espin expression during development is initiated by the activity of specific HC fate and differentiation genes. Transduction of nonsensory inner ear cells with the transcription factor ATOH1 induces the formation of HC-like cells, some of which will form stereocilia, although they are often immature.[13,18] ATOH1 overexpression has also been shown to induce stereociliagenesis in damaged HCs, although again some such stereocilia are immature.[28] Therefore ATOH1 alone does not appear to be sufficient to specify appropriate *espn* gene expression. ATOH1 is known to directly regulate the gene encoding the HC differentiation transcription factor POU4F3,[29] and animals that lack the *pou4f3* gene fail to develop stereocilia.[30] It is thus possible that POU4F3 directly regulates the *espn* gene. We therefore evaluated the 1500 bp region 5' to the start site of the murine *espn* gene for consensus POU4F3 binding sites, as identified by Xiang et al.,[31] or the JASPAR database. Two sites were found ~650–800 bp 5' to the *espn* transcription initiation site. This provides suggestive, but by no means sufficient, evidence of POU4F3 regulation. In any case, low levels of expression of POU4F3, or of other HC differentiation factors, may explain the insufficient *espn* transcription in damaged and regenerated HCs.

Differentiated HCs express Notch, and the Notch pathway inhibits adjacent supporting cells from differentiating into HCs.[32–34] Lin et al.[19] reported that HC regeneration was promoted by Notch inhibition, with conversion of supporting cells to HCs and increased *atoh1* transcriptional activity. This is consistent with our results in which many more Myosin7A-positive cells were observed in damaged epithelia that were treated with DAPT. In our study, we did not observe stereociliary bundles on the myosin7A-positive cells induced by Notch inhibition alone (data not shown) within 7days. This suggests that Notch signaling may not be sufficient for complete development of HCs, which might otherwise be expected if Notch effects are mediated by increased ATOH1. Alternatively, stereocilliary regeneration induced by Notch inhibition may require additional time.

In conclusion, espin1 gene therapy appears be useful for significantly enhancing morphological and physiological stereociliary bundle regeneration on damaged and

regenerated HCs. The combination of Notch inhibition and espin1 gene transduction is therefore a promising candidate for inner ear regenerative therapy in future. However, it must be noted that our experiments were performed in neonatal mice. Future studies will be needed to determine whether this regenerative effect occurs in adult mice, a necessary pre-requisite for potential clinical utility.

MATERIALS AND METHODS

Animals

CD-1 mice of both sexes were purchased from Japan SLC Inc., Hamamatsu, Japan and bred under standard husbandry conditions. They were housed under SPF conditions in rodent boxes on sawdust bedding. Pups were used at 2 days after birth. Experimental protocols were approved by the Animal Research Committee of Kyoto University Graduate School of Medicine and complied with the US National Institutes of Health Guidelines for the Care and Use of Laboratory Animals.

Production of Ad-espin vectors

Replication-deficient recombinant adenoviruses with deleted E1, E3, and E4 regions 18 were used. Expression plasmids containing cDNAs for the Espin1-EGFP conjugate (Espin1-EGFP) and the Espin4-EGFP conjugate were kindly provided by Prof. James Bartles of Northwestern University. Adenovirus Espin1-EGFP (Ad-E1) and adenovirus Espin4-EGFP (Ad-E4) were constructed using the Adenovirus Expression Vector Kit Ver. 2 (Takara) according to the manufacturer's protocol. In brief, the Espin1 or Espin4 cDNAs were transferred to a cosmid shuttle vector (pAxCAwtit, Takara) containing the human cytomegalovirus promoter and SV40 termination sequence, and amplified. Then they were linearized by restriction enzyme digest. The expression inserts were transferred to the pAdEasy-1 adenoviral vector[35] by electroporation. The adenoviruses vectors were amplified in human embryonic kidney cells (HEK-293, RIKEN Bioresource Center, Cell No. RCB1637) and purified with the Adeno-X Maxi purification Kit (Clontech). We employed the vectors at a concentration of 1×10^7 total particles of purified virus per milliliter (pfu/ml). Viral suspensions were kept at –80°C until thawed for use. Appropriate protein production by Ad.E1-EGFP and Ad.E4-EGFP was confirmed by Western blotting following transduction of fibroblasts.

Dissection of vestibular maculae and tissue culture

Postnatal mice were decapitated under deep anesthesia and their temporal bones were removed. Utricula maculae were dissected from the surrounding tissue in 0.01M phosphate-buffered saline, pH 7.4. The otoconial membranes were gently removed with a fine needle. Explants of utricular sensory epithelia were placed intact on type I collagen-coated cover glasses (Iwaki, Tokyo, Japan) and maintained in 24-well culture plates (Iwaki) in Dulbecco's modified Eagle's medium (Invitrogen, Eugene, Oregon, USA), supplemented with 6 g/l glucose (Wako Pure Chemicals, Osaka, Japan) and 1.5 g/l penicillin G (Wako Pure Chemicals), at 37°C in a humidified atmosphere of 95% air and 5% CO_2 for 24 hrs.

In order to examine the toxicity of gentamicin (GM) to HC stereociliary bundles and HC bodies, we damaged explants with 1mM GM (Nakarai, Japan) for 48 hrs and then maintained the explants in culture without GM for 10 days. After fixation with 4% paraformaldehyde and histochemistry (see below), we counted stereociliary bundles and HC bodies. Bundles and HC bodies were measured using a 10 × 40 eyepiece reticule. Each square of the reticule was 100 μm on a side. Surviving hair bundles and HC bodies were counted in each of three randomly selected fields including both striolar and extrastriolar regions, and the values obtained were averaged. Means and SDs were then converted into percentages for illustration in the figure. Five utricles were examined in each condition (n=5), based on our prior experience with treatment variability.

Effect of notch inhibition

To induce HC-like cells, two days after GM damage, we cultured utricular explants with 20 μM DAPT (N-[N-[(3,5-Difluorophenyl)acetyl]-L-alanyl]-L-phenylglycinetert-butyl : $C_{23}H_{26}F_2N_2O_4$, Abcam) for 2 days, followed by 5 days without DAPT. DAPT is a prototypical γ-secretase inhibitor. Since Notch signaling requires γ-secretase activity, DAPT is a potent inhibitor of this signaling pathway. As a control, we cultured GM-damaged utricles for 7 days without DAPT. Explants were analyzed for myosin7A immunoreactivity both as whole mounts and as tissue sections

Transduction of Ad-espins

Utricular maculae were cultured in DMEM overnight and then damaged with GM for two days. On the third day, we transduced 5 explants each with Ad-E1 or Ad-E4 (1×10^7 pfu/ml) overnight. Using the same conditions, we transduced adenovirus GFP (Ad-GFP) as a control. Explants were then cultured in DMEM for 7 days. For Notch inhibition, DAPT (20μM) was applied for 2 days, in between GM damage and adenovirus transduction.

Observation GFP expression using time-lapse microscopy

Beginning 70 hrs after adenovirus transduction, we evaluated GFP expression using time-lapse microscopy (BZ9000, Keyence, Japan). Each of the five samples was observed three times per hr (20 mins) from 24 hrs after transduction up to 70 hrs. This method was used to identify the time of maximal GFP-adenoviral expression.

Histochemical analysis

At the end of the culture period, explants were fixed for 15 min in 4% paraformaldehyde and permeabilized with 5% Triton X-100 in phosphate-buffered saline (PBS) after 3X PBS wash. Explants were then exposed to a blocking solution containing 10% bovine serum albumin (BSA), and then incubated with anti- myosin7A rabbit polyclonal antibodies (25–6790; Proteus Bioscience Inc., Ramona, CA, USA; 1:500). Alexa-Fluor 568 goat anti-rabbit IgG (A-11011, Invitrogen, CA, USA; 1:100) was used as the secondary antibody. At the same time, specimens were incubated in FITC-conjugated or Alexa-Fluor 633 phalloidin (1:100; Invitrogen) to label F-actin for 1 hr. Finally, the explants were incubated with DAPI for 15 min. Specimens were examined using a Leica TCS-SP2 laser-scanning confocal microscope (Leica Microsystems Inc., Wetzlar, Germany). Cells with phalloidin-positive

surface structures were counted in randomly selected areas and averaged in each sample for each condition, using an evaluation reticule 100 μm on each side. Results from 6–7 samples were evaluated, based on initial observations of variability.

Observation of stereociliary bundles by scanning electron microscopy (SEM)

After the elimination of most stereociliary bundles by GM exposure, the process of hair bundle re-emergence induced by *espin* transduction was assessed by SEM. The explants were fixed with 4% paraformaldehyde and 0.05% glutaraldehyde at 4°C for 4 hrs. After fixation, they were dehydrated, dried, and coated with a thin layer of platinum palladium. The specimens were examined with a Hitachi S-4700 scanning electron microscope (Hitachi, Tokyo, Japan). Structures which exhibited clear stereociliary characteristics were counted in standard, randomly selected areas and averaged for each condition (n=6–8 explants, based on the variability exhibited by explants). Each square of the evaluation reticule employed was 30 μm on each side.

Functional analysis with FM1–43FX

To evaluate the physiological function of surviving HCs, we exposed GM-treated, DAPT exposed and transfected explants to FM1–43 (3-[4-[2-[4-(dibutylamino)phenyl]ethenyl] pyridin-1-ium-1-yl]propyl-triethylazanium dibromide: $C_{30}H_{49}Br_2N_3$) FX dye (5μM, Invitrogen). FM1–43 is a lipophilic, fluorescent dye that passes very rapidly through the MET channels located on HC stereociliary bundles. For this reason, HC fluorescence after brief exposure to FM1–43 is commonly used to verify the functional status of the cells. The explants were transferred to culture media supplemented with 5 μM FM1–43 for 10 seconds. During FM1–43 incubation, we applied mechanical stimulation via a fluid stream from a pipette, as described previously.[36] After fixation with 4% PFA, the specimens were examined with a TCS-SP2 laser-scanning confocal microscope. Three independent assays were performed in each condition. FM1–43 positive cells were counted in randomly selected areas and averaged for each condition (n=6–9, based on prior studies). Each square of the evaluation reticule was 100 μm on each side.

Statistical analysis

Sample sizes were chosen based on our prior experience with variability in GN-exposed macular explants, to detect substantial differences in the measured variables. Samples were excluded from the experiments if they failed to attach to the culture surface or were folded. Because all samples were essentially identical, no randomization was performed. Analysis was unblinded. Statistical analysis was performed by analysis of variance (ANOVA) followed by the least significant difference (LSD) post-hoc test with Bonferroni correction for repeated measures and two-sided t-test (Stat View 5.0), after determination of normal distribution and comparable variances between samples. Differences associated with P values of less than 0.05 were considered to be statistically significant. All data are presented as mean ± standard deviation (SD).

ACKNOWLEDGMENTS

We thank Prof. James Bartles (Northwestern University) for kindly providing plasmids encoding espin1 and espin4 conjugated to EGFP. This research was supported by a Health and Labor Science Research Grant for Research on Specific Disease (Vestibular Disorders) from the Ministry of Health, Labor and Welfare, Japan (2014), a Grant-in-Aid for Scientific Research from the Ministry of Education, Science, Sports, Culture and Technology of Japan, and grant BX001205 from the Veterans Administration of the United States. The ARRIVE guidelines were followed in experimental design and completion, as well as manuscript preparation.

REFERENCES

1. Nadol JB Jr. Hearing loss. N Engl J Med. 1993; 329:1092–1102. [PubMed: 8371732]
2. Roberson DF, Weisleder P, Bohrer PS, Rubel EW. Ongoing production of sensory cells in the vestibular epithelium of the chick. Hear Res. 1992; 57:166–174. [PubMed: 1733910]
3. Ryals BM, Rubel EW. Hair cell regeneration after acoustic trauma in adult Coturnix quail. Science. 1988; 240:1774–1776. [PubMed: 3381101]
4. Gale JE, Meyers JR, Periasamy A, Corwin JT. Survival of bundleless hair cells and subsequent bundle replacement in the bullfrog's saccule. J Neurobiol. 2002; 50:81–92. [PubMed: 11793356]
5. Jia S, Yang S, Guo W, He DZ. Fate of mammalian cochlear hair cells and stereocilia after loss of the stereocilia. J Neurosci. 2009; 29:15277–15285. [PubMed: 19955380]
6. Sekerková G, Zheng L, Loomis PA, Mugnaini E, Bartles JR. Espins and the actin cytoskeleton of hair cell stereocilia and sensory cell microvilli. Cell Mol Life Sci. 2006; 63:2329–2341. [PubMed: 16909209]
7. Sekerkov G, Zheng L, Mugnaini E, Bartles JR. Differential expression of espin isoforms during epithelial morphogenesis, stereociliogenesis and postnatal maturation in the developing inner ear. Dev. Biol. 2006; 291:83–95. [PubMed: 16413524]
8. Li H, Liu H, Balt S, Mann S, Corrales CE, Heller S. Correlation of expression of the actin filament-bundling protein espin with stereociliary bundle formation in the developing inner ear. J. Comp. Neurol. 2004; 468:125–134. [PubMed: 14648695]
9. Rzadzinska A, Schneider M, Noben-Trauth K, Bartles JR, Kachar B. Balanced levels of Espin are critical for stereociliary growth and length maintenance. Cell Motil Cytoskeleton. 2005; 62:157–165. [PubMed: 16206170]
10. Zheng L, Sekerková G, Vranich K, Tilney LG, Mugnaini E, Bartles JR. The deaf jerker mouse has a mutation in the gene encoding the espin actin-bundling proteins of hair cell stereocilia and lacks espins. Cell. 2000; 102:377–385. [PubMed: 10975527]
11. Van de Water TR, Staecker H, Halterman MW, Federoff HJ. Gene therapy in the inner ear. Mechanisms and clinical implications. Ann N Y Acad Sci. 1999; 884:345–360. [PubMed: 10842605]
12. Ryan AF, Dazert S. Gene therapy for the inner ear: challenges and promises. Adv Otorhinolaryngol. 2009; 66:1–12. [PubMed: 19494569]
13. Kawamoto K, Yagi M, Stover T, Kanzaki S, Raphael Y. Hearing and hair cells are protected by adenoviral gene therapy with TGF-beta1 and GDNF. Mol. Ther. 2003; 7:484–492. [PubMed: 12727111]
14. Kawamoto K, Sha SH, Minoda R, Izumikawa M, Kuriyama H, Schacht J, et al. Antioxidant gene therapy can protect hearing and hair cells from ototoxicity. Mol Ther. 2004; 9:173–181. [PubMed: 14759801]
15. Izumikawa M, Minoda R, Kawamoto K, Abrashkin KA, Swiderski DL, Dolan DF, et al. Auditory hair cell replacement and hearing improvement by Atoh1 gene therapy in deaf mammals. Nat Med. 2005; 11:271–276. [PubMed: 15711559]
16. Schlecker C, Praetorius M, Brough DE, Presler RG Jr, Hsu C, Plinkert PK, et al. Selective atonal gene delivery improves balance function in a mouse model of vestibular disease. Gene Ther. 2011; 18:884–890. [PubMed: 21472006]
17. Tona Y, Hamaguchi K, Ishikawa M, Miyoshi T, Yamamoto N, Yamahara K, et al. Therapeutic potential of a gamma-secretase inhibitor for hearing restoration in a guinea pig model with noise-induced hearing loss. BMC Neurosci. 2014; 15:66. [PubMed: 24884926]

18. Mizutari K, Fujioka M, Hosoya M, Bramhall N, Okano HJ, Okano H, et al. Notch inhibition induces cochlear hair cell regeneration and recovery of hearing after acoustic trauma. Neuron. 2013; 77:58–69. [PubMed: 23312516]
19. Lin V, Golub JS, Nguyen TB, Hume CR, Oesterle EC, Stone JS. Inhibition of Notch activity promotes nonmitotic regeneration of hair cells in the adult mouse utricles. J Neurosci. 2011; 31:15329–15339. [PubMed: 22031879]
20. Ahmed M, Xu J, Xu PX. EYA1 and SIX1 drive the neuronal developmental program in cooperation with the SWI/SNF chromatin-remodeling complex and SOX2 in the mammalian inner ear. Development. 2012; 139:1965–1977. [PubMed: 22513373]
21. Atkinson PJ, Huarcaya Najarro E, Sayyid ZN, Cheng AG. Sensory hair cell development and regeneration: similarities and differences. Development. 2015; 142:1561–1571. [PubMed: 25922522]
22. Ryan AF. The cell cycle and the development and regeneration of hair cells. Curr Topics Devel Biol. 2002; 57:449–466.
23. Loomis PA, Zheng L, Sekerková G, Changyaleket B, Mugnaini E, Bartles JR. Espin cross-links cause the elongation of microvillus-type parallel actin bundles in vivo. J Cell Biol. 2003; 163:1045–1055. [PubMed: 14657236]
24. Rzadzinska A, Schneider M, Noben-Trauth K, Bartles JR, Kachar B. Balanced levels of Espin are critical for stereociliary growth and length maintenance. Cell Motil Cytoskeleton. 2005; 62:157–165. [PubMed: 16206170]
25. Gale JE, Marcotti W, Kennedy HJ, Kros CJ, Richardson GP. FM1–43 dye behaves as a permeant blocker of the hair-cell mechanotransducer channel. J Neurosci. 2001; 21:7013–7025. [PubMed: 11549711]
26. Meyers JR, MacDonald RB, Duggan A, Lenzi D, Standaert DG, Corwin JT, et al. Lighting up the senses: FM1–43 loading of sensory cells through nonselective ion channels. J Neurosci. 2003; 23:4054–4065. [PubMed: 12764092]
27. Griesinger CB, Richards CD, Ashmore JF. FM1–43 reveals membrane recycling in adult inner hair cells of the mammalian cochlea. J Neurosci. 2002; 22:3939–3952. [PubMed: 12019313]
28. Yang SM, Chen W, Guo WW, Jia S, Sun JH, Liu HZ, et al. Regeneration of stereocilia of hair cells by forced Atoh1 expression in the adult mammalian cochlea. PLoS One. 2012; 7:e46355. [PubMed: 23029493]
29. Masuda M, Dulon D, Pak K, Mullen LM, Li Y, Erkman L, et al. Regulation of POU4F3 gene expression in hair cells by 5' DNA in mice. Neuroscience. 2011; 197:48–64. [PubMed: 21958861]
30. Erkman L, McEvilly RJ, Luo L, Ryan AK, Hooshmand F, O'Connell SM, et al. Role of transcription factors Brn-3.1 and Brn-3.2 in auditory and visual system development. Nature. 1996; 381:603–606. 1996. [PubMed: 8637595]
31. Xiang M, Zhou L, Macke JP, Yoshioka T, Hendry SH, Eddy RL, et al. The Brn-3 family of POU-domain factors: primary structure, binding specificity, and expression in subsets of retinal ganglion cells and somatosensory neurons. J Neurosci. 1995; 15:4762–4785. [PubMed: 7623109]
32. Yamamoto N, Tanigaki K, Tsuji M, Yabe D, Ito J, Honjo T. Inhibition of Notch/RBP-J signaling induces hair cell formation in neonate mouse cochleas. J Mol Med (Berl). 2006; 84:37–45. [PubMed: 16283144]
33. Hori R, Nakagawa T, Sakamoto T, Matsuoka Y, Takebayashi S, Ito J. Pharmacological inhibition of Notch signaling in the mature guinea pig cochlea. Neuroreport. 2007; 18:1911–1914. [PubMed: 18007185]
34. Murata J, Ikeda K, Okano H. Notch signaling and the developing inner ear. Adv Exp Med Biol. 2012; 727:161–173. [PubMed: 22399346]
35. He TC, Zhou S, da Costa LT, Yu J, Kinzler KW, Vogelstein B. A simplified system for generating recombinant adenoviruses. Proc Natl Acad Sci U S A. 1998; 95:2509–2514. [PubMed: 9482916]
36. Taura A, Kojima K, Ito J, Ohmori H. Recovery of hair cell function after damage induced by gentamicin in organ culture of rat vestibular maculae. Brain Res. 2006; 1098:33–48. [PubMed: 16764839]

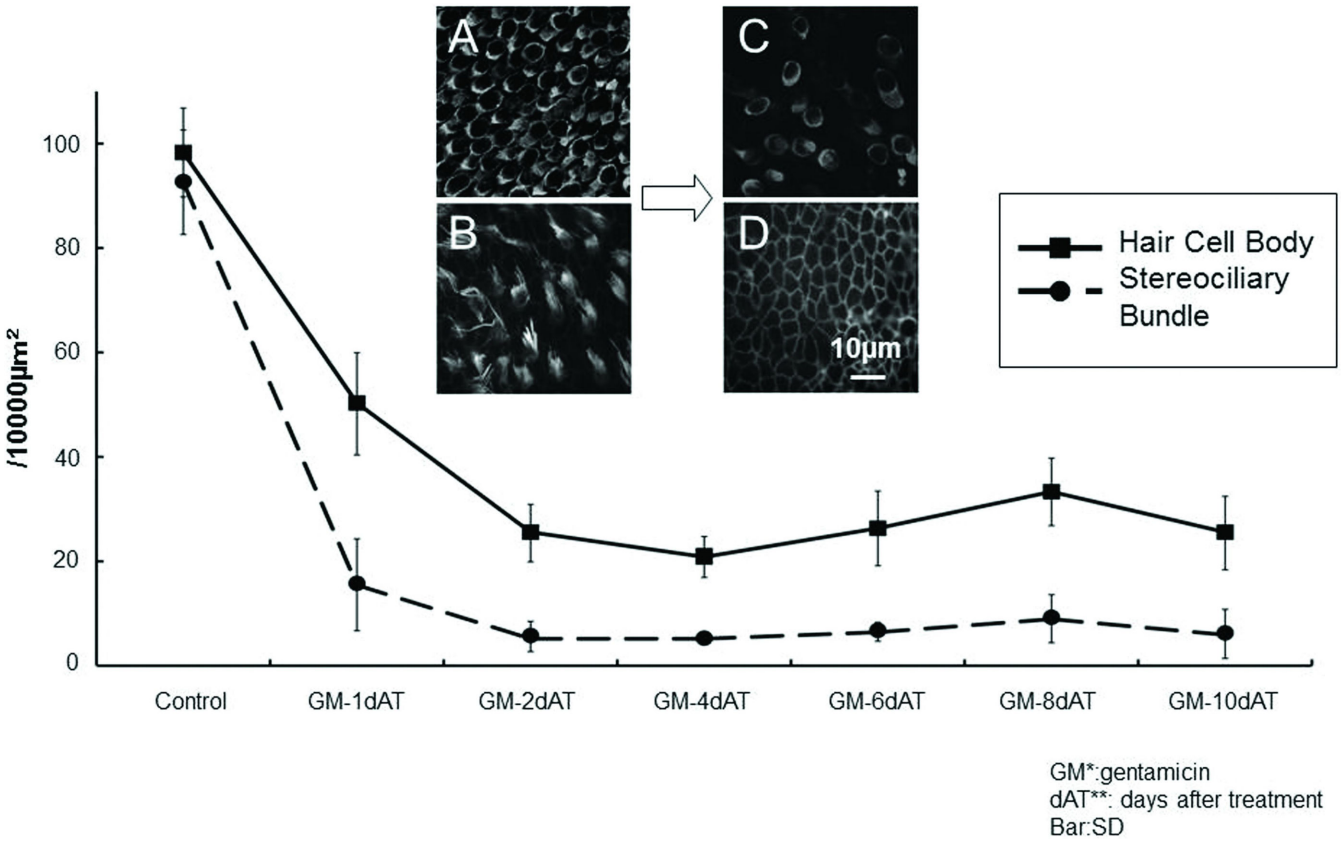

Figure 1.

Number of stereociliary bundles and HC bodies after GM treatment. **A**: control (myosin7A), **B**: control (phalloidin), **C**: GM 10d AT (myosin7A), **D**:GM 10d AT (phalloidin). After GM treatment, almost all hair bundles are lost, and the number of HC bodies decreases. However, some HCs without hair bundles remain even 10 days after damage (n=5 explants/time). Points represent means and bars represent SD (standard deviation).

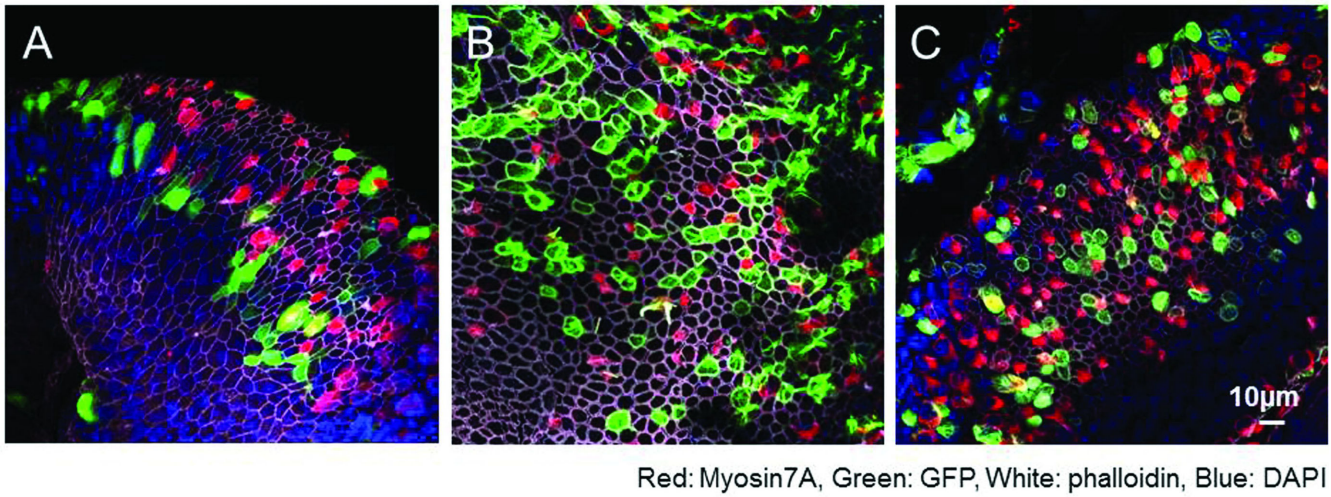

Figure 2.

Adenoviral transduction after GM treatment. **A**: After Ad-GFP transduction, GFP expression was diffused throughout the cell body. **B**: After Ad-E1 transduction, a filamentous pattern of GFP expression was observed. **C**: After Ad-E4 transduction, a filamentous pattern of GFP expression was also observed. Most GFP positive cells were negative for Myosin7A (Red), suggesting that the majority of transduced cells were supporting cells. Red: Myosin7A, Green: EGFP, White: phalloidin, Blue: DAPI.

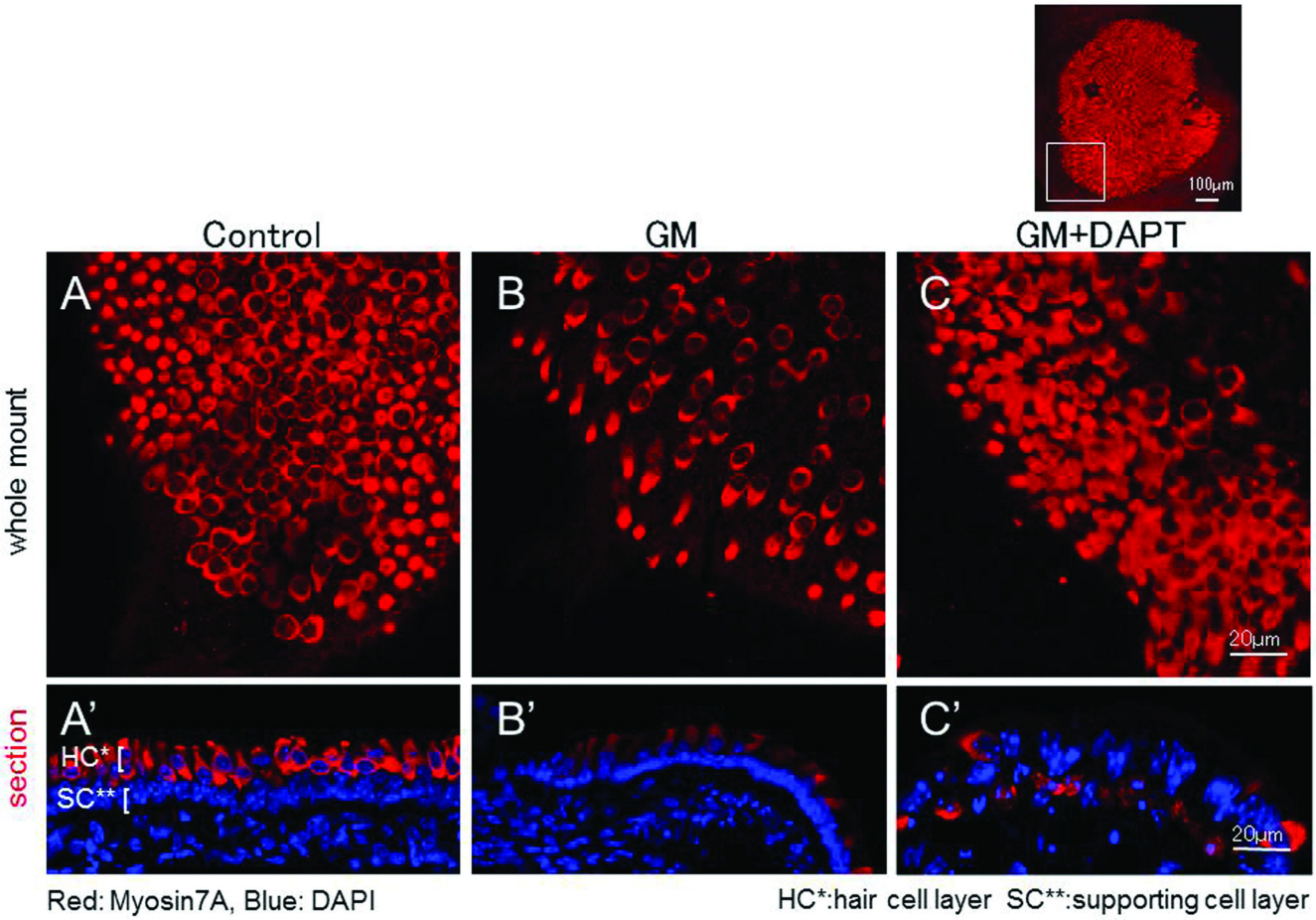

Figure 3.

The effects of DAPT exposure after GM treatment. **A, A':** control explant (2 days culture). HCs are densely present. **B, B':** Two days after GM treatment. HCs decreased dramatically. **C, C':** DAPT application after GM treatment. Many myosin7A-positive cells were observed. In a tissue section, myosin7A-positive cells were numerous in the supporting cell layer (arrows). A–C: whole mount. A'-C': section. Red: Myosin7A, Blue: DAPI. HC*: HC layer SC**: supporting cell layer.

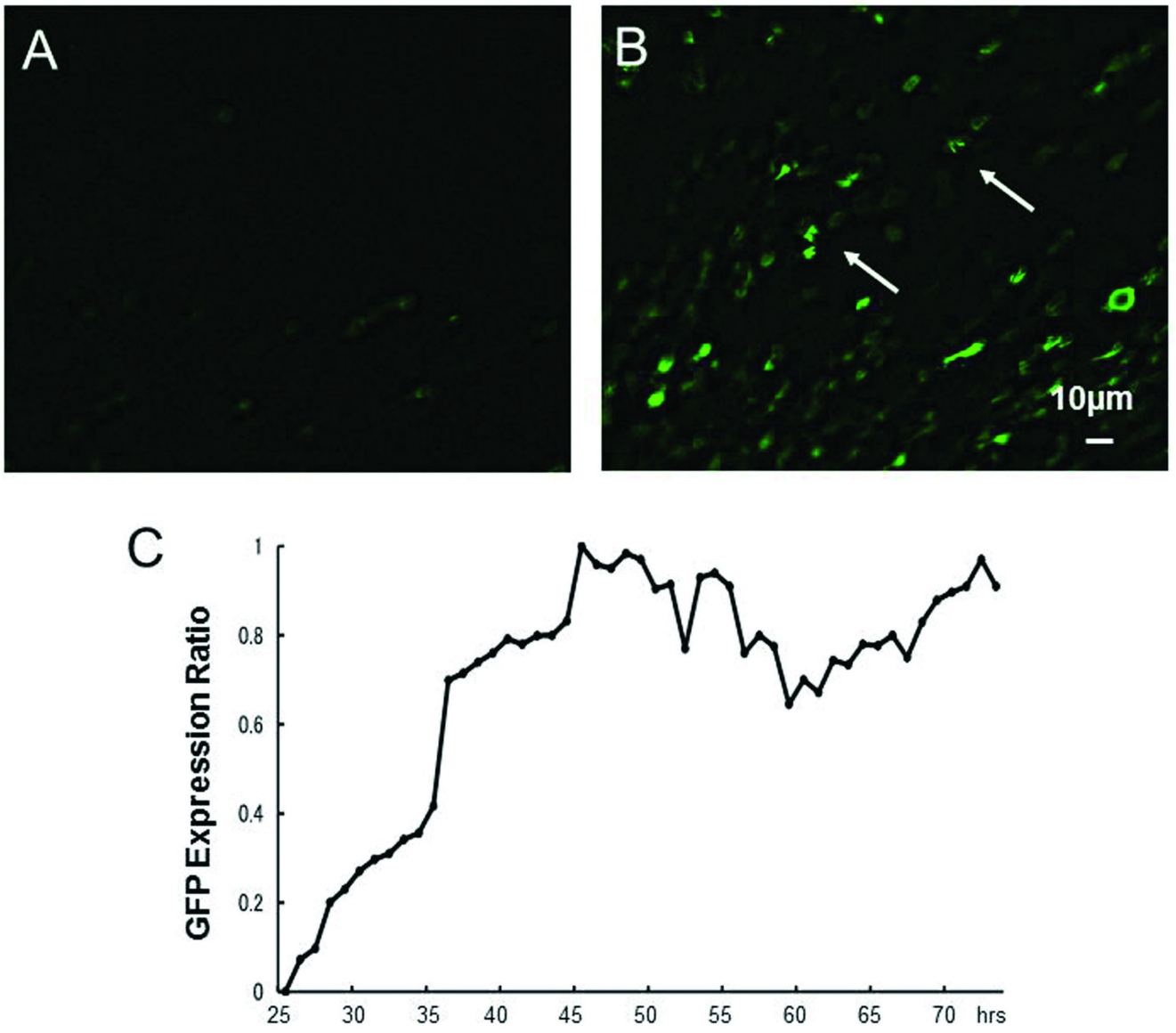

Figure 4.

Time course of GFP expression after adenoviral transduction. **A**: Twenty-four hrs after Ad-E1 administration. **B**: Forty-eight hours after Ad-E1 administration. Filamentous GFP expression was observed (arrows). **C**: Intensity ratio of GFP expression for a typical explant. Adenoviral GFP expression is maximal 46 hrs after adenovirus administration.

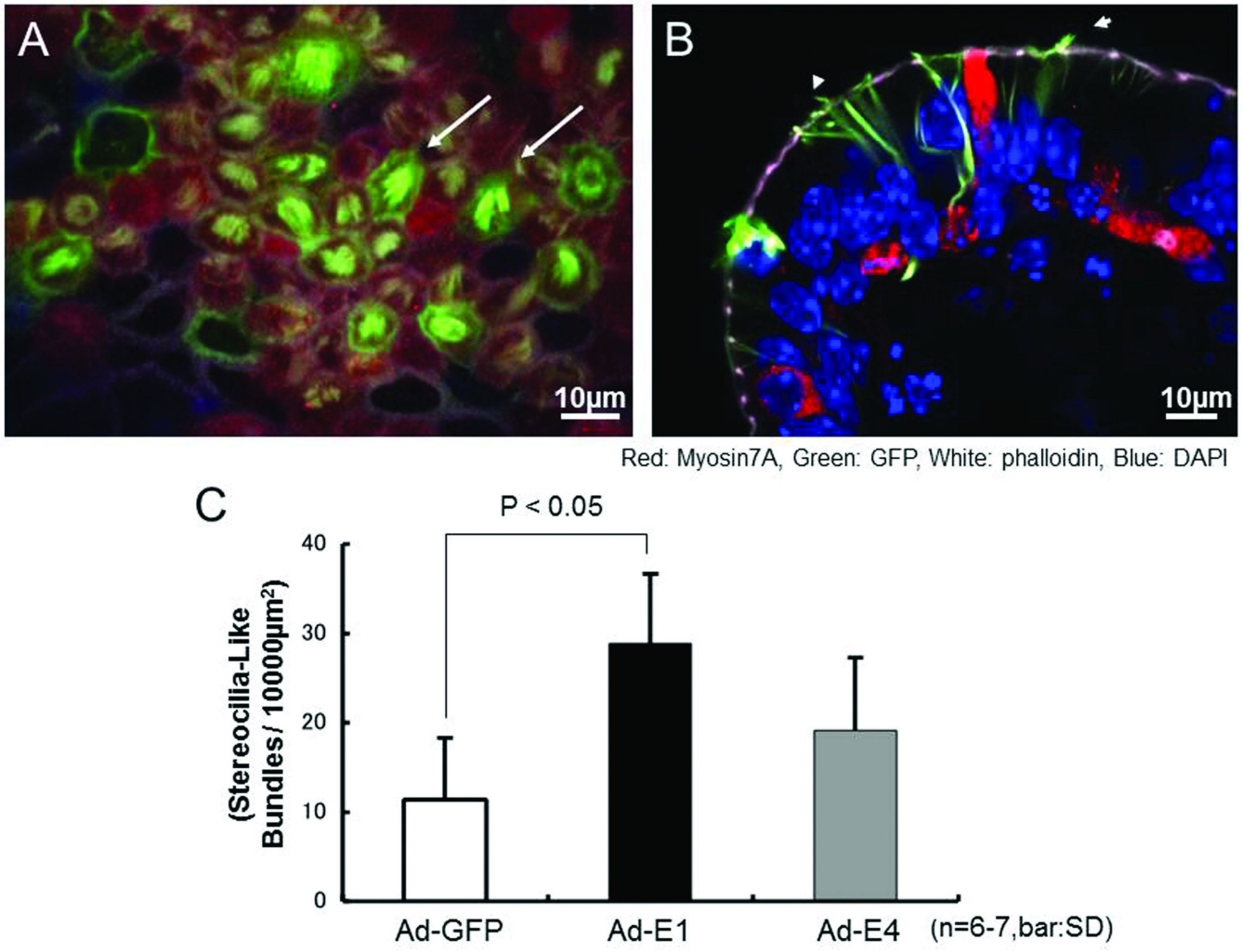

Figure 5.

Hair bundle-like structures on Ad-E1 transduced explants. **A:** Whole mount utricular explant. Many myosin7A-positive cells with hair-bundle-like structures on their apical surfaces are observed (e.g. arrows). **B:** Sectioned explant. Myosin7A-positive cell bodies are observed in the supporting cell layer. Hair-bundle-like structures protrude from extensions of these cells that reach the apical surface of the epithelium (e.g. arrowhead). Red: Myosin7A; Green: EGFP; Blue: DAPI. **C:** Number of hair-bundle-like structures observed after adenoviral transduction. In Ad-GFP transduced explants, a few damaged stereociliary bundles remained. However, in Ad-E1 transduced explants, there are many more immature hair bundles. In Ad-E4 transduced explants, some filamentous cilia-like structures are observed. The number of bundle-like structures in Ad-E1 transduced explants was significantly greater than in control (Ad-GFP) explants than in Ad-GFP transduced explants ($p < .05$, 6–7 explants per group)..

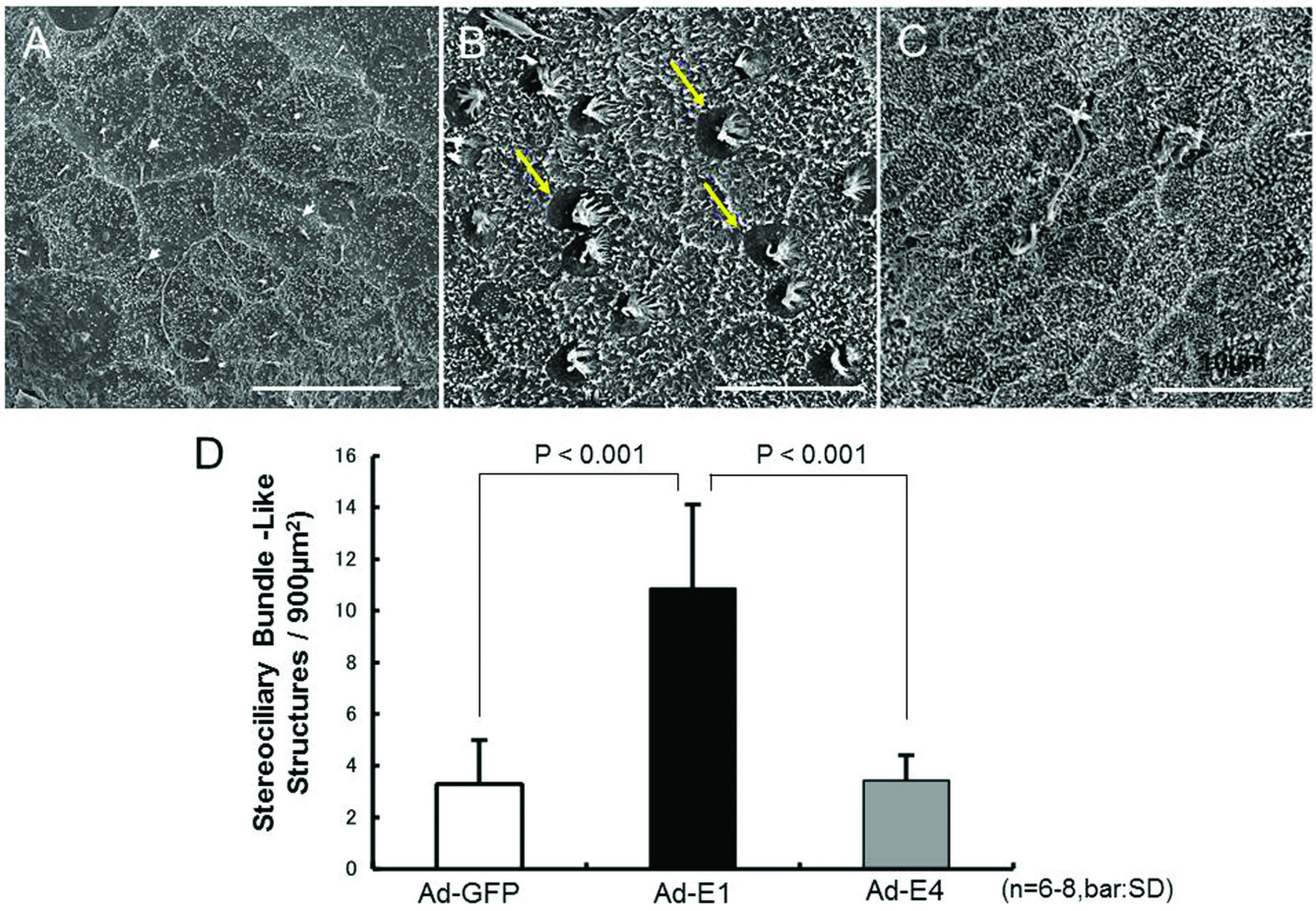

Figure 6.

Scanning electron microscopy (SEM) analysis. A–C: Representative explants. **A:** Ad-GFP transduction. Reticulated cell borders are observed. Some damaged hair bundles and basal bodies (e.g. arrowheads) remain, but few structures resembling stereocilliary arrays are present. **B:** Ad-E1 transduced explants. Many apparently immature hair-bundle-like structures are observed (e.g. arrows). **C:** Ad-E4. Extended microvillus-like structures and microvilli are apparent. There are some damaged streociliary bundles, but few immature hair-bundle-like structures are apparent. **D.** Quantitative analysis: Number of streociliary bundle-like structures in SEM. Significantly more of these structures are observed on Ad-E1 transduced explants, than on those transduced with Ad-GFP or Ad-E4 ($P < .001$; 6–8 explants per treatment condition).

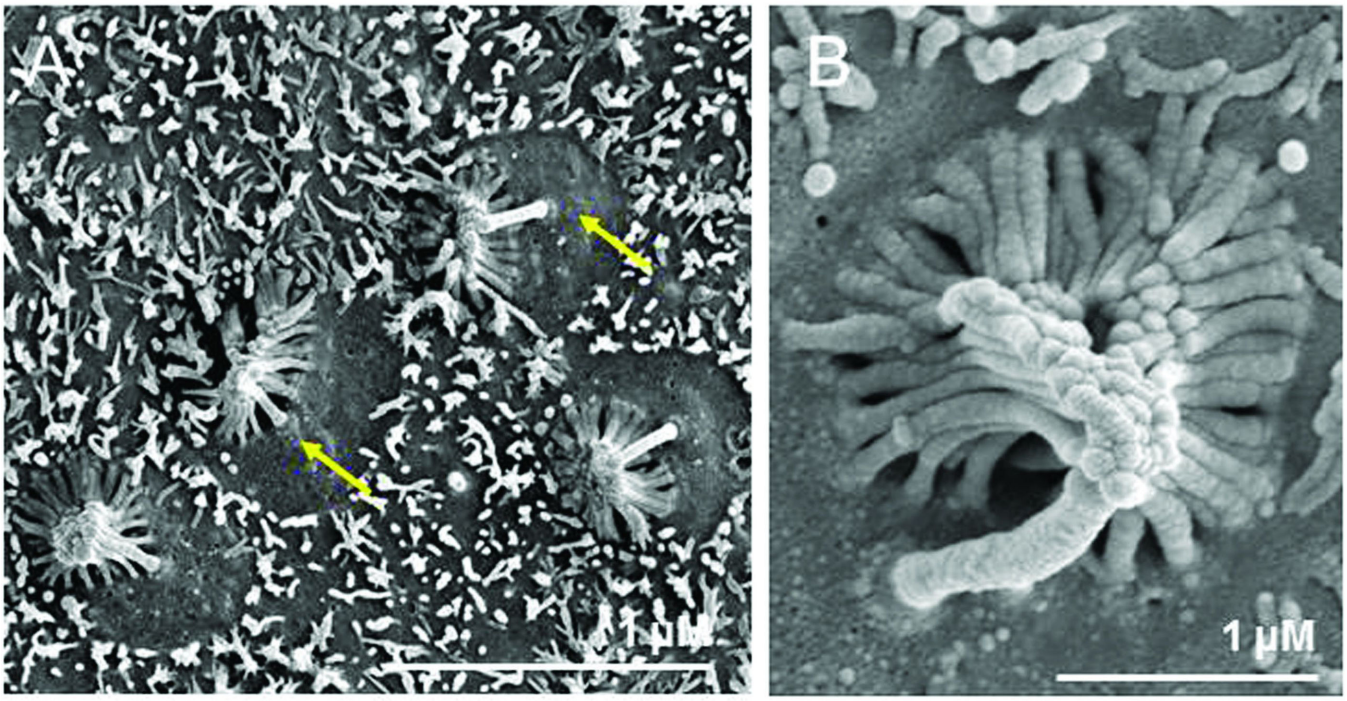

Figure 7.

High magnification of Ad-E1 transduction in SEM observation. **A**: In each cell, one kinocilium is observed in the center of the cell and stereocilia are present on approximately half of the apical surface. **B**: Stereocilia exhibit a staircase pattern. The upper ends of the stereocilia appear to adhere to one another.

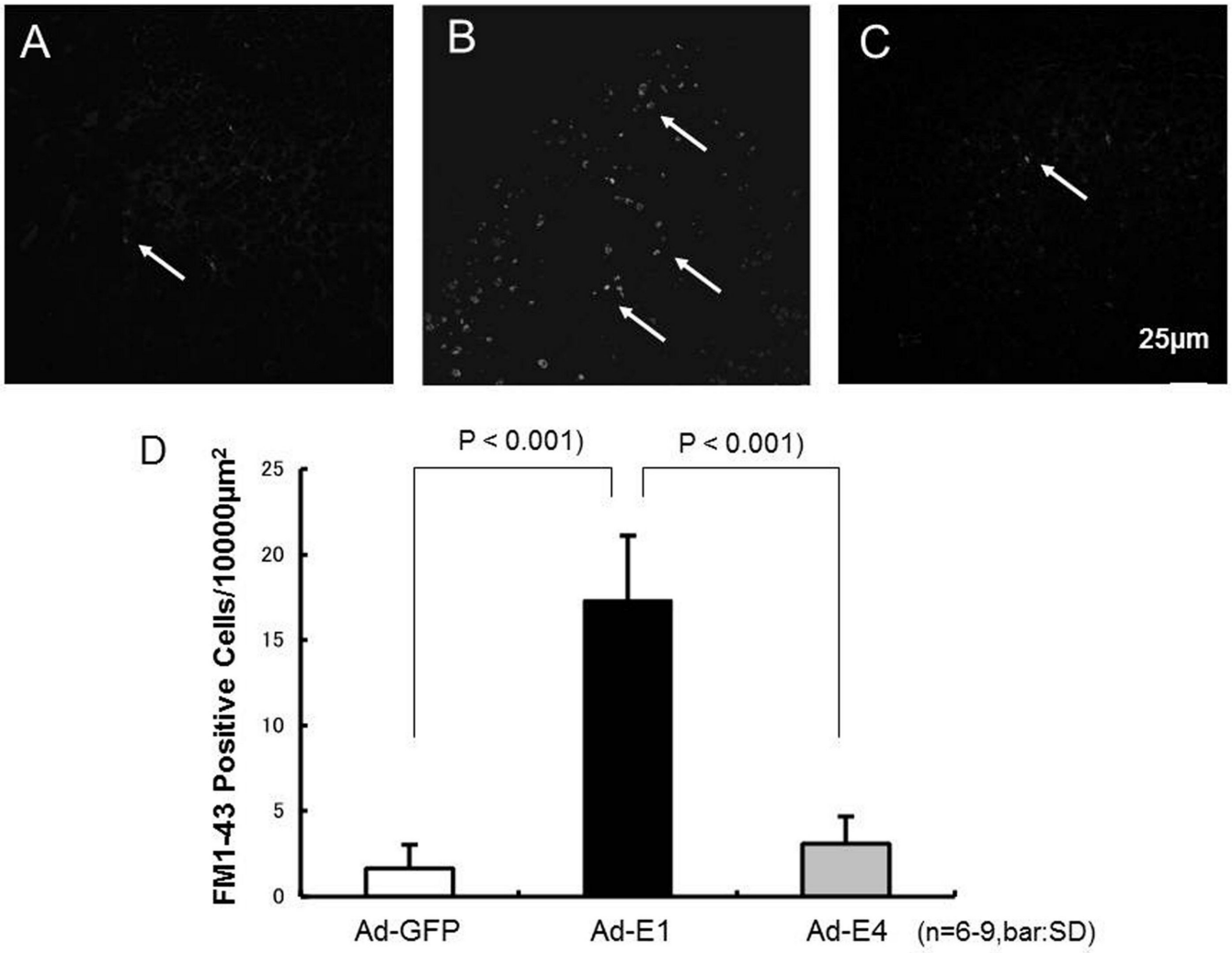

Figure 8.

Functional analysis of stereociliary bundles using FM1–43FX. **A**: Ad-GFP transduced explants. **B**: Ad-E1 transduced explants. **C**: Ad-E4 transduced explants. Only a few FM1–43 positive cells, as indicated by fluorescent labeling, are observed in A and C. In contrast, many more FM1–43 positive cells are seen in B (arrows). **D:** Quantitative FM1–43 analysis. In Ad-E1 transduced explants, there are a number of FM1–43-loaded cells. However, FM1–43 positive cells are much less prevalent in Ad-GFP and Ad-E4 explants. These differences were significant ($P < .05$, 6–9 explants per treatment condition).